Superconducting Circuits and Quantum Computation

Academic and Research Staff
Professor Terry P. Orlando

Postdoctoral Students
Dr. Yang Yu, Dr. Jonathan Habif

Collaborators
Prof. Leonid Levitov, Prof. Seth Lloyd, Prof. Johann E. Mooij[1], Dr. Juan J. Mazo[2], Dr. Fernando F. Falo[2], Prof. Karl Berggren, Prof. M. Tinkham[4], Dr. Nina Markovic[4], Dr. Sergio Valenzuela[4], Prof. Marc Feldman[5], Prof. Mark Bocko[5], Dr. Enrique Trías, Dr. William Oliver[3], Dr. Zachary Dutton[6]

Visiting Scientists and Research Affiliates
Dr. Juan Mazo[2], Prof. Johann E. Mooij[1], Dr. Kenneth J. Segall[7], Dr. Enrique Trías

Graduate Students
Donald S. Crankshaw, Daniel Nakada, Murali Kota, Janice Lee, Bhuwan Singh, David Berns, William Kaminsky, Bryan Cord

Undergraduate Students
Andrew Clough

Support Staff
Jacques Wood

Introduction

Superconducting circuits are being used as components for quantum computing and as model systems for non-linear dynamics. Quantum computers are devices that store information on quantum variables and process that information by making those variables interact in a way that preserves quantum coherence. Typically, these variables consist of two quantum states, and the quantum device is called a quantum bit or qubit. Superconducting quantum circuits have been proposed as qubits, in which circulating currents of opposite polarity characterize the two quantum states. The goal of the present research is to use superconducting quantum circuits to perform the measurement process, to model the sources of decoherence, and to develop scalable algorithms. A particularly promising feature of using superconducting technology is the potential of developing high-speed, on-chip control circuitry with classical, high-speed superconducting electronics. The picosecond time scales of this electronics means that the superconducting qubits can be controlled rapidly on the time scale and the qubits remain phase-coherent.

Superconducting circuits are also model systems for collections of coupled classical non-linear oscillators. Recently we have demonstrated a ratchet potential using arrays of Josephson junctions as well as the existence of a novel non-linear mode, known as a discrete breather. In addition to their classical behavior, as the circuits are made smaller and with less damping, these non-linear circuits will go from the classical to the quantum regime. In this way, we can study the classical-to-quantum transition of non-linear systems.

---

[1] Delft University of Technology, The Netherlands
[2] University of Saragoza, Spain
[3] M.I.T. Lincoln Laboratory
[4] Harvard University
[5] University of Rochester
[6] NIST, Gaithersburg
[7] Colgate University

1. Superconducting Persistent Current Qubits in Niobium

Sponsors

Project Staff

Dr. Yang Yu, Daniel Nakada, Dr. Jonathan Habif, Donald Crankshaw, Dr. Kenneth Segall, Bhuwan Singh, Janice C. Lee, Murali Kota, Bryan Cord, and Dr. Sergio Valenzuela (Harvard); Professors Terry Orlando, Karl Berggren, Leonid Levitov, Seth Lloyd and Professor Michael Tinkham (Harvard), Dr. William Oliver (MIT Lincoln Laboratory)

Quantum Computation combines the exploration of new physical principles with the development of emerging technologies. In these beginning stages of research, one hopes to accomplish the manipulation, control and measurement of a single two-state quantum system while maintaining quantum coherence between states. This requires a coherent two-state system (a qubit) along with a method for control and measurement. Superconducting quantum computing has the promise of an approach that could accomplish this in a manner that can be scaled to a large numbers of qubits. We are studying the properties of a two-state system made from a niobium (Nb) superconducting loop, which can be incorporated on-chip with other superconducting circuits for control and measurement. The devices we study are fabricated at MIT Lincoln Laboratory, which uses a Nb-trilayer process for the superconducting elements and optical projection photolithography to define circuit features. Our system is inherently scalable but has the challenge of being able to demonstrate appreciable quantum coherence.

The particular device under study is made from a loop of Nb interrupted by three Josephson junctions (Fig. 1a). The application of an external magnetic field to the loop induces a circulating current whose magnetic field either enhances (circulating current in the clockwise direction) or subtracts (counterclockwise) from the applied magnetic field. When the applied field is near one-half of a flux quantum Φ_0, both the clockwise and counterclockwise current states are classically stable. The system behaves as a two-state system. The potential energy versus circulating current is a so-called double-well potential, with the two minima representing the two states of equal and opposite circulating current.
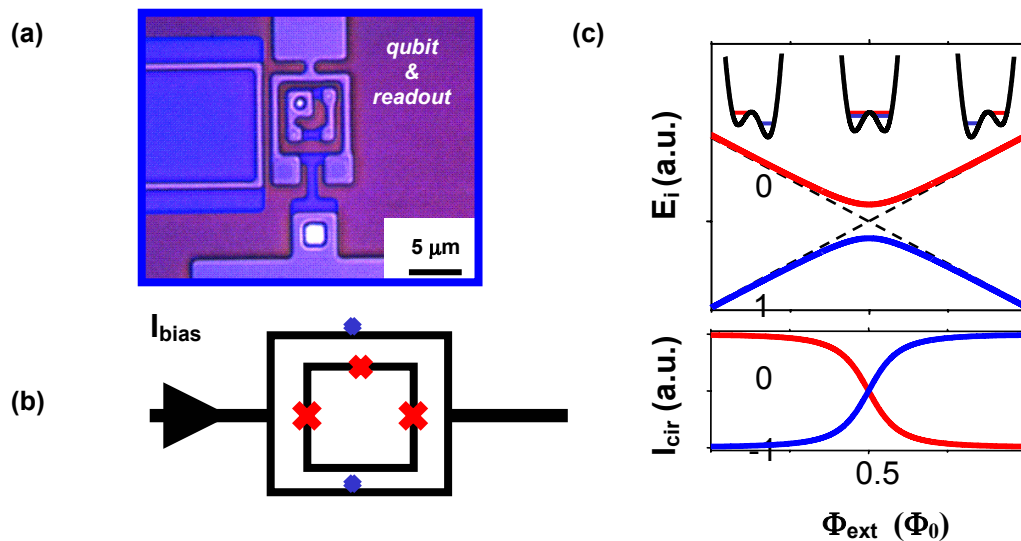

Figure 1: **(a)** SEM image of the persistent current qubit (inner loop) surrounded by the measuring dc SQUID. **(b)** A schematic of the persistent current qubit and measuring SQUID, the **x** mark the Josephson junctions. **(c)** The energy levels for the ground state (dark line) and the first excited state of the qubit versus applied flux Φ_{ext}. The double well potentials are shown schematically above. The lower graph shows the circulating current in the qubit for both states as a function of applied flux (in units of flux quantum Φ_0).

Figure 1a shows a SEM image of the persistent current qubit (inner loop) and the measuring dc SQUID (outer) loop. A schematic of the qubit and the measuring circuit is shown in Figure 1b, where the Josephson junctions are denoted by **x**'s. The sample is fabricated at MIT Lincoln Laboratory in niobium by photolithographic techniques on a trilayer of niobium-aluminum oxide-niobium.

The energy levels of the ground state (dark line) and the first excited state (light line) are shown in Figure 1c near the applied magnetic field of 0.5 Φ_0 in the qubit loop. Classically the Josephson energy of the two states would be degenerate at this bias magnetic field and increase or decrease linearly from this bias field, as shown by the dotted line. Since the slope of the *E* versus magnetic field is the circulating current, we see that these two classical states have opposite circulating currents. However, quantum mechanically, the charging energy couples these two states and results in an energy level repulsion at Φ_{ext} = 0.5 Φ_0, so that there the system is in a linear superposition of the currents flowing in opposite directions. As the applied field is changed from below Φ_{ext} = 0.5 Φ_0 to above, we see that the circulating current goes from negative, to zero at Φ_{ext} = 0.5 Φ_0, to positive as shown in the lower graph of Figure 1c. This flux can be measured by the sensitive flux meter provided by the dc SQUID.

A SQUID magnetometer inductively coupled to the qubit is used to measure the change in magnetic field caused by the circulating current and thus determine the state of the qubit. The SQUID has a switching current which depends sensitively on magnetic field. When the magnetic field from the qubit adds to the external field we observe a given switching current value; when it subtracts from the external field we observe a slightly larger switching current value. We measure the switching current by ramping up the bias current of the SQUID and recording the current at which it switches to the finite voltage state. Typically a few hundred measurements are taken at a given magnetic field to determine the state of the qubit.

2. DC Measurements of Macroscopic Quantum Levels in a Superconducting Qubit Structure with a Time-Ordered Meter

Sponsors

Project Staff
Donald Crankshaw, Dr. Kenneth Segall, Daniel Nakada, Bhuwan Singh, Janice Lee, Dr. William Oliver and Dr. Sergio Valenzuela; Professors Terry Orlando, Karl Berggren, Leonid Levitov, Seth Lloyd and Michael Tinkham

The persistent-current qubit has a double-well potential, with the two minima corresponding to magnetization states of opposite sign. Macroscopic resonant tunneling between the two wells is observed at values of energy bias that correspond to the positions of the calculated quantum levels. The magnetometer, a Superconducting Quantum Interference Device (SQUID), detects the state of the qubit in a time-ordered fashion, measuring one qubit state before the other. This results in a different meter output depending on the initial state, providing different signatures of the energy levels for each tunneling direction. From these measurements, the intrawell relaxation time is inferred to be ~ 50 μs. This is in agreement with direct experimental measurements of the energy relaxation time τ_d between macroscopic quantum states.
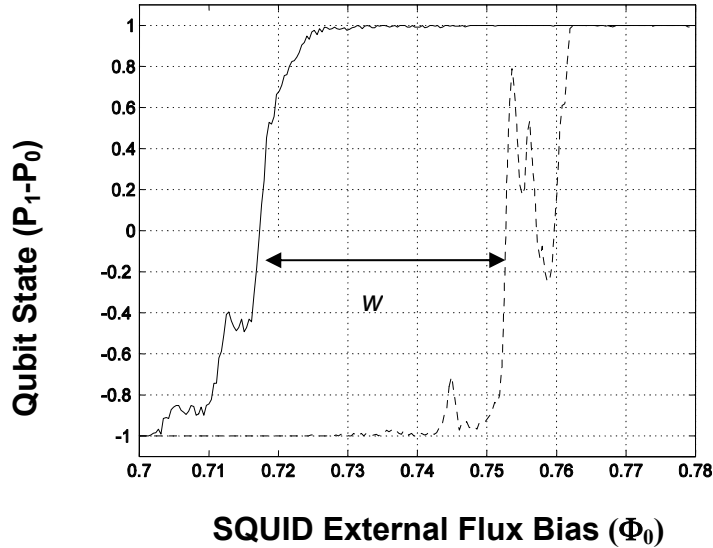
Figure 1: (a) Measured probability of the system being in state **1** minus the probability of being in state **0** for given external flux bias. The plot shows the proportion of switching events where the qubit is measured in the **1** state minus the proportion found in the **0** state (P_1-P_0). The solid line is for a qubit prepared in the **1** state. The dotted line shows the measured qubit state when it is prepared in the **0** state. The dotted line shows numerous peaks and dips, while the solid line's structure is less pronounced.

Figure 1 shows the probability of the system being in state **1** minus the probability of being in state **0**. The measurement is performed at 15 mK and is hysteretic, depending on the initial preparation state of the system. The plot shows the proportion of switching events where the qubit is measured in the **1** state minus the proportion where it is found in the **0** state (P_1-P_0) against the magnetic flux bias of the dc SQUID in units of flux quanta (f_S). The solid line is for a qubit prepared in the **1** state, represented in the double-well diagram as a solid circle. The dashed line shows the measured qubit state when it is prepared in the **0** state. The dashed line shows numerous peaks and dips, while the solid line's structure is less pronounced. The width of the hysteresis is labeled in Figure 1 with a *w*. As the temperature increases, the hysteresis loop closes. The width of the hysteresis loop *w* versus temperature is nearly constant for low temperatures, and nearly linear for higher temperatures.
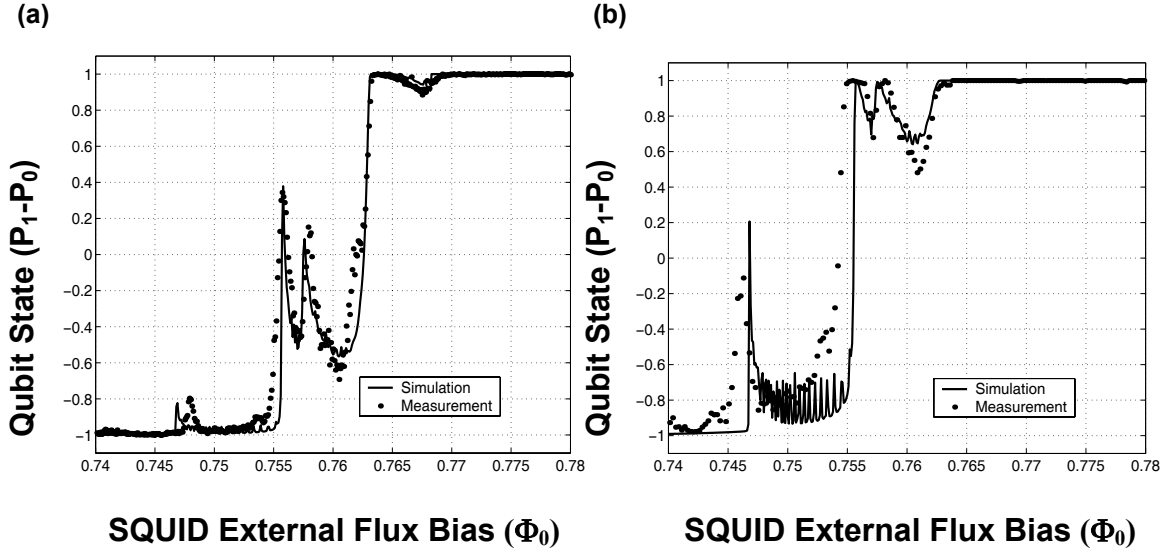
(a)

(b)

Figure 2: Qubit state P_1-P_0 when the SQUID is ramped at a rate of **(a)** 60 Hz and **(b)** 12.5 Hz. The solid lines correspond to the theoretical model, while the solid dots are experimental data points. The slower ramp rate results in a higher probability that the qubit will transition to the **1** state, as is made clear by the growing peaks marked by the vertical lines.

Figure 2 shows the qubit state when the SQUID is ramped at a rate of 60 Hz and 12.5 Hz. The simulation of the flux ramps shown in the figures, produce a match between the theoretical model and experiment measurements at two different ramp rates. The solid lines correspond to the theoretical model, while the solid circles are experimental data points. The two show good agreement. The slower ramp rate at 12.5Hz results in a higher probability that the qubit will transition to the **1** state, as is made clear by the growing peaks. The oscillations in (b) between f_S=.748 and .755 are artifacts of the numerical simulation. Fits to this data suggest an intra-well relaxation time of the order of 50 μs.

3. Energy Relaxation Time between Macroscopic Quantum Levels in a Superconducting Persistent Current Qubit

Sponsor

Project Staff

Professor Terry Orlando, Dr. Yang Yu, Daniel Nakada, Janice C. Lee, Bhuwan Singh, Donald Crankshaw, Dr. William Oliver (MIT Lincoln Laboratory), Professor Karl K. Berggren

We demonstrated spectroscopy and measured the intrawell relaxation time τ_d 24 μs in a Nb persistent-current (PC) qubit. The dissipation, which results from the coupling between the qubits and the environment, was then determined from τ_d. The decoherence time for Superconducting qubits (SQs), including energy and phase relaxation times, is predicted to be proportional to the level of dissipation. Therefore, we estimated that, for our configuration with a Nb superconducting qubit, the decoherence time is about 20 μs within the spin-boson model by assuming an ohmic environment.

The samples were fabricated at MIT Lincoln Laboratory in a Nb trilayer process. The critical currents of the Josephson junctions in the qubit are 1.2 µA and 0.75 µA, respectively. The critical currents of the junctions are relatively large so the qubit has multi-levels in one of the potential wells [Fig.1 (b)]. Spectroscopy of the qubit energy levels was achieved using micro-wave pulses to produce photon induced transitions (PIT). For each measurement trial, we first prepared the qubit in state **1**. Microwaves with duration time t_{pul} were then applied, inducing transitions between states **1** and **0**. After the microwaves were shut off, the qubit state (**0** or **1**) was then read out from the switching current I_{sw} of the readout dc SQUID. This procedure was repeated more than 10^3 times to minimize the statistical error. Shown in Fig. 2 are contour plots of the switching-current histograms obtained by scanning the frustration at T = 15 mK. Each vertical slice is a histogram of I_{sw}, and the color represents the number of switching events. The lower branch represents the qubit in the **0** state, and the upper branch represents the qubit in the **1** state. The left-most tip of the higher branch marked a fixed frustration point. The most striking feature of the contour plots is that a population "gap" (i.e., zero population region) in the **1** branch was created by the microwaves (Fig. 2 (b) to (d)). With increasing microwave frequency, the gap moved away from the tip, as expected from the energy level structure. We believe that the PIT here was an incoherent process, because the microwave pulse duration was much longer than the estimated decoherence time.
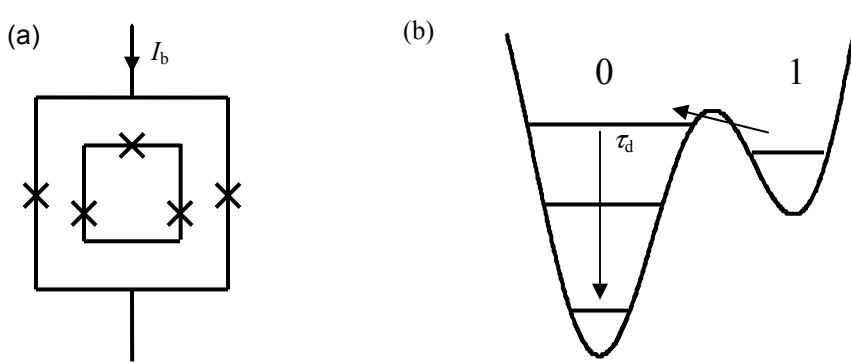

Figure 1: (a) Schematic of the PC qubit surrounded by a readout dc SQUID. **(b)** Schematic of the qubit's double-well potential with multi-energy levels in one well. Microwaves pump the qubit from the lowest level of **1** to the excited level of **0**, then decay to the ground level of **0** with a time scale τ_d.
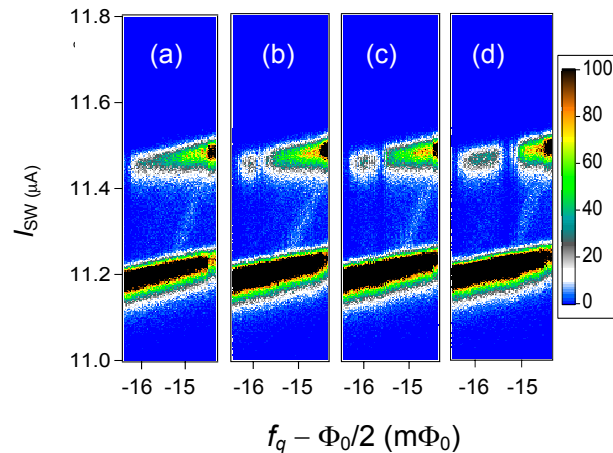

Figure 2: Contour plots of the switching current distribution **(a)** without microwaves, and with microwaves at **(b)** ν = 6.77 GHz, **(c)** 7.9 GHz, and **(d)** 9.66 GHz.

Additionally, no periodic variation of population with varying pulse duration was observed. In a simple two-level system, observing such a gap would be unexpected for an incoherent transition, since the population in the lower level should always be larger than 0.5 in that case. In order to address this gap phenomenon in our multi-level system, a multi-level pump-decaying model is introduced. The qubit remaining in the state **1** is then approximately given by

$$P_1(t) \approx a_1 e^{-t/\tau'}, \tag{1}$$

where a_1 can be considered as a constant in the relevant time scale, $\tau' \approx 2\tau_d$ for large microwave power. We can see with t sufficient long, $P_1(t) \rightarrow 0$; this agrees with the experimental observations. From Eq. 1, we can determine τ_d by measuring $P_1(t)$. Because I_{sw} of **0** is smaller than that of **1**, pumping the system from state **1** to state **0** will generate a dip in I_{sw} average vs. frustration, and the dip amplitude is proportional to $1-P_1$. Fig. 3 (a) shows the dip amplitude as a function of the microwave irradiation time, t_{pul}. τ' can be determined by a best fit. We then cranked microwave power and found τ' saturates at about 50 µs [Fig .3 (b)]. We then obtained τ_d
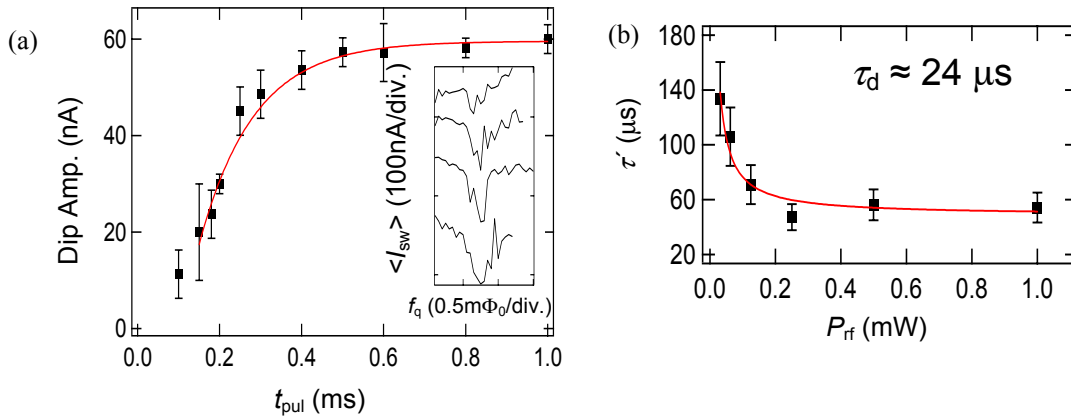
24.3 µs from a best fit.

Figure 3: (a) The amplitude of the microwave resonant dip as a function of microwave duration t_{pul}. The microwave frequency ν = 9.66 GHz, and nominal power P_{rf} = 31.3 µW. The solid squares are experimental data and the line is a best fit to an exponential decay. The inset shows the resonant dips at t_{pul} = 0.2, 0.5, 0.8 and 1 ms, from the top to the bottom. **(b)** τ' vs. microwave power for ν = 9.66 GHz.

This long intrawell relaxation time is important for experiments in QC in two ways. First, the lower two energy levels in the left well could themselves be used as the two qubits states, with a third state used as the readout state. Because our PC qubit had no leads directly connected to it, the PC qubit is much less influenced by its environment than are other similar single-junction schemes. Second, if we assume that the environment can be modeled as an ohmic bath, as in the spin-boson model, we can estimate the decoherence time of a PC qubit in which the qubit states are those of opposite circulating current. For our Nb PC qubit operating with opposite circulating currents states, a conservative estimate gives the decoherence time is about 20 µs at 15 mK.

4. Resonant Readout of a Persistent Current Qubit with SQUID Josephson Inductance

Project Staff
Janice C. Lee, Dr. William Oliver (MIT Lincoln Laboratory), Professor Terry Orlando

The two logical states of a persistent current (PC) qubit correspond to oppositely circulating currents in the qubit loop. The induced magnetic flux associated with the current either adds to or subtracts from the background flux. The state of the qubit can thus be detected by a DC SQUID magnetometer inductively coupled to the qubit.

One way to read out the qubit state is to measure the value of the switching current of the DC SQUID (fig. 1). One typically ramps a bias current through the SQUID and record the current value at which it switches to the voltage state. Depending on the state of the qubit, the SQUID senses a different magnetic flux and has different switching current values.   This existing approach requires a high current bias, and the switching action can generate many quasi-particles; both of which are undesired and can shorten the decoherence time of the qubit.
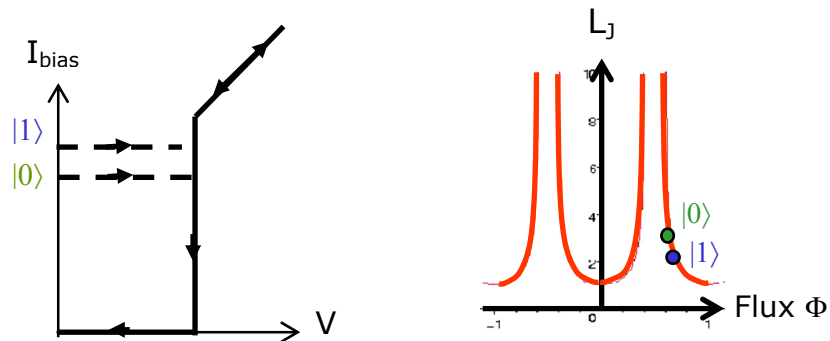

Figure 1 (left): Typical IV trace of an underdamped DC SQUID. The switching current value is different depending on the qubit state. **Figure 2 (right):** The Josephson inductance of a DC SQUID is a function of magnetic flux and can also be used to differentiate the qubit states.

This report describes an alternative measurement scheme which detects the state of the qubit by measuring the Josephson inductance of the readout SQUID. Like the switching current, the Josephson inductance of the SQUID is also a periodic function of the flux that it senses and thus is different for the two qubit states (fig. 2).   To measure the Josephson inductance with high sensitivity, the SQUID is inserted in a high Q resonant circuit (fig. 3). For illustrative purpose, a simple RLC circuit is shown instead of the actual high-Q resonant circuit that was designed for the experiment. The resonant frequency f_o of the circuit is related to the Josephson inductance L_J by $1/2\pi\sqrt{L_J C}$. A transition between the two qubit states manifests itself as a shift in resonant frequency (fig. 4). This new inductance measurement approach requires the SQUID be biased only at low current values along the supercurrent branch, offering an advantage over the conventional switching current measurement method which inherently drives the SQUID to its normal state.
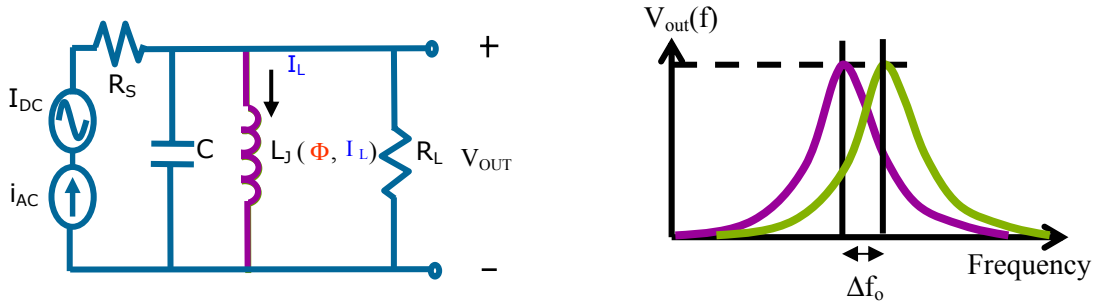
Figure 3 (left): The Josephson inductance can be determined with high sensitivity by inserting the SQUID in a resonant circuit and measuring the resonant frequency. The current bias values are kept below the critical current of the SQUID. **Figure 4 (right):** A transition between the qubit states is detected as a shift in resonant frequency.

Figure 5 shows the typical frequency spectrum of the SQUID readout circuit measured experimentally at 300mK. The resonant frequency was designed to be near 420MHz, with a high Q on the order of a thousand. Notice that the shape of the spectrum was asymmetric, with the peak leaning towards the low frequency side. Such a shape is characteristic to non-linear circuits, and was observed here due to the fact that the SQUID Josephson inductance is nonlinear in nature and depends on the size of the SQUID current bias. Figure 6 shows the modulation of the resonant frequency (from the SQUID Josephson inductance) by an external magnetic field. The discrete jump corresponds to a transition between the two qubit states.
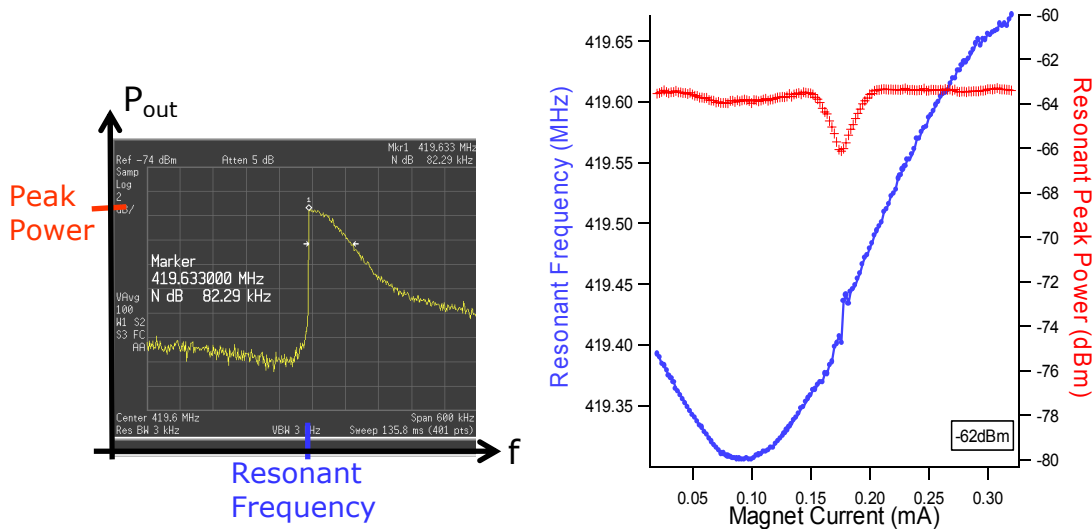

Figure 5 (left): Typical frequency spectrum of the non-linear SQUID resonant circuit measured experimentally at 300mK. The resonant peak occurs at near 420MHz, with a Q on the order of a thousand. **Figure 6 (right):** The bottom curve (left axis) shows the modulation of the resonant frequency with an external magnetic field. The shift in resonant frequency corresponds to a transition between the two qubit states. The top curve (right axis) shows the amplitude of the peak power. Note that a dip in power was observed at the qubit step.

5. Fast On-Chip Control Circuitry

Sponsors

Project Staff

Dr. Jonathan Habif and Professor Karl Berggren (MIT), Professor Marc Feldman and Professor Mark Bocko (University of Rochester)

Preparation, manipulation and measurement of a quantum bit must be performed with classical circuitry. It is necessary that the classical circuitry be fast on the time scale of the qubit operation time, and provide an environment sufficiently quiet that its presence will not significantly decrease the qubit coherence time. Superconducting rapid single flux quantum (RSFQ) electronics utilizes the fundamental quantum of magnetic flux associated with superconductors as digital data bits. Using Josephson junction circuit elements the single flux quanta (SFQ) data travel between gates as transient voltage with picosecond pulse widths. A plot of the traveling data pulse is shown in Fig. 1. Digital logic circuits are constructed with RSFQ so that the magnetic data bits can be directed to interact with the magnetic-flux based persistent-current qubit (pc-qubit) to perform the necessary classical operations to drive a quantum bit.
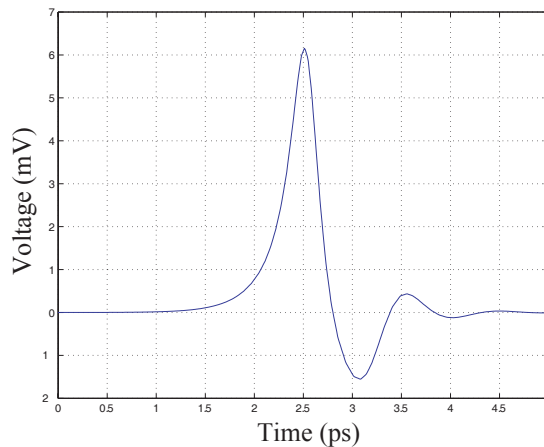

Figure 1: A transient, SFQ data pulse used as a data bit in RSFQ circuits.

The first example of such a general digital circuit for quantum coherent manipulation was fabricated at MIT Lincoln Laboratory, designed and successfully tested by collaborators at the University of Rochester. A schematic of the circuit is shown in Figure 2. The control circuit is comprised of three distinct elements, the Josephson transmission line (JTL), the destructive readout (DRO), and the flux comparator. The JTL is responsible for shuttling the ultra-fast data pulses between digital logic gates. The data pulses are sent from gate to gate as transient voltages with characteristic frequencies of 100's of GHz, and the JTLs maintain the sharp timing of the pulses preventing dispersion. The DRO acts as a one bit memory element with two inputs, the first for providing the data to be stored, the second for purging data stored in the DRO. Since the data is stored in the DRO as a stable persistent supercurrent the flux can be inductively coupled to the pc-qubit thereby rapidly enhancing or canceling flux applied to the qubit externally.

Therefore, the DRO can be utilized to initialize the state of the qubit by modulating the qubit potential localizing the system wavefunction, and can also be used to drive the system by providing a sharp, non-adiabatic 'kick' to the system rapidly exciting the qubit with flux. The flux comparator consists of a superconducting SQUID ring inductively coupled to the pc-qubit.

When a transient SFQ pulse is presented to the input of the comparator the comparator passes the pulse to its output only if the flux coupled to its interior is greater than a threshold value. The flux comparator can be used to make a digital measurement of the state of the pc-qubit on the timescale of the transient SFQ pulse.
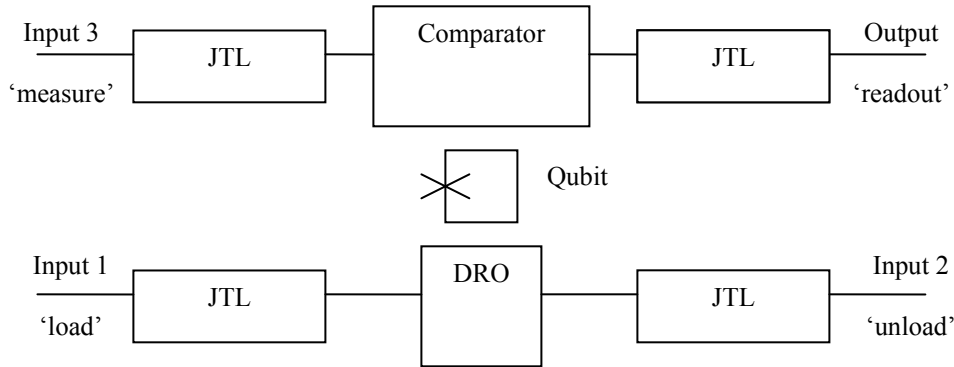

Figure 2: An RSFQ circuit for arbitrary operation on a single superconducting flux-based quantum bit.

The circuit shown in Figure 1 is designed to perform all of these functions in order to systematically initialize, manipulate and measure the qubit. At 'input 1' a SFQ data pulse is supplied to be stored in the DRO as a persistent current and serves to modulate the magnetic field applied to the qubit localizing the quantum mechanical probability amplitude of the system. Sending a second data pulse to 'input 2' quickly annihilates the data stored in the DRO, thereby modulating the potential landscape of the system and exciting the qubit to a higher energy state where it can undergo free oscillations of its probability amplitude. The wavefunction of the system oscillates between the computational basis states at the frequency corresponding to the quantum energy level splitting. The time that the system is allowed to freely oscillate can be engineered to yield single qubit gate operations. After a predetermined time a data pulse is presented to 'input 3' and the comparator rapidly interrogates the flux state of the qubit, relaying the result of the measurement to the 'output'. Since the data pulses and digital logic gates operate at frequencies near 100 GHz, and the free oscillation frequency of the system is in the regime of single gigahertz, it is feasible to precisely engineer and control the state of a flux qubit using RSFQ circuitry.

The circuit shown in Figure 1 indicates complete functionality of the separate operations necessary for quantum coherent manipulation of a superconducting qubit. The technology in which the circuit was fabricated, however, is not conducive to the fabrication of quantum bits with useful coherence times. Therefore, the circuit will be rescaled to meet the parameters of a foundry process accommodating both the quantum coherent circuitry and the digital RSFQ circuitry. The successful interfacing of a single flux qubit with RSFQ circuitry provides impetus to examine efficient scaling strategies for controlling a quantum processor with RSFQ. The penultimate goal of this work is to generate a general purpose architecture that can be scaled with seamlessly with the scaling of a quantum computer.

6. Design of Coupled Qubit

Project Staff
Bhuwan Singh, Dr. Jonathan Habif, Professor Terry Orlando

Quantum computing requires the ability to manipulate individual qubits as well as coupled qubits. The type of coupling used depends on the physical implementation of the qubit. One such physical implementation is the Persistent-current (PC) qubit. A PC qubit is a superconducting loop interrupted by three Josephson junctions, of which two are the same size and one is slightly smaller. The two different quantum states ($|0\rangle$ and $|1\rangle$) of a PC qubit correspond to current circulating in opposite directions. These oppositely circulating currents produce flux in opposite directions. Since the computational states of a PC qubit are stored in its induced flux degree of freedom, the simplest way of coupling two PC qubits together is through a flux-based interaction. In this approach, two PC qubits are coupled together through mutual inductive coupling. The schematic for the layout is shown in Fig. 1. The central requirement for a coupled qubit system is that the 4 computational states – $|00\rangle$, $|01\rangle$, $|10\rangle$, and $|11\rangle$ – be experimentally distinguishable through measurement. For a single PC qubit, its state is measured by a DC SQUID. The DC SQUID can detect the difference in flux produced by the $|0\rangle$ or $|1\rangle$ states. The basic idea is unchanged for the coupled qubit system. In this case, there is one DC SQUID that measures the collective state of the coupled qubits through the total induced flux created by both qubits. For example, the $|00\rangle$ state would have qubits 1 and 2 both having counterclockwise circulating current. Alternately, the $|11\rangle$ state would have both qubits with clockwise circulating current. If the individual qubits were measurable with the DC SQUID, then the $|00\rangle$ and $|11\rangle$ states of the coupled qubit system would also be measurable because the total flux induced on the DC SQUID is simply the sum of the individual qubit fluxes. The difficulty in measurement comes in differentiating the $|01\rangle$ and $|10\rangle$ states. For these states, the two individual qubits have flux in opposite directions. If the two qubits were identical in all aspects, it would be impossible to distinguish these two states. In fact, these two states would no longer be eigenstates of the coupled qubit Hamiltonian. In order to create a difference in the measured flux between the $|01\rangle$ and $|10\rangle$ states, the two qubits are fabricated to have differing circulating current magnitudes. The magnitude of the circulating current is determined by the size of the junctions in the PC qubit.

Apart from being measurable, the four qubit states must have appropriate energy level spacing. The requirement on energy level spacing is a result of the operational mode of the qubit. Individual qubit rotations as well as coupled qubit operations, such as CNOT, are achieved through applied RF radiation of the appropriate frequency. For one, there must be no degeneracy of energy levels for the 4-state coupled qubit system. There are six transitions defined among these four states. For a practical quantum computer, it is desired that each of these six transitions has sufficiently unique energy level spacing. In this case, "sufficient" is determined by the thermal broadening of the energy levels at the operational temperature as well as the linewidth of the external or on-chip oscillator. If this condition is met, then external RF pulses could be used to do universal quantum computation on the 2-qubit system. To meet this requirement on the energy levels, the qubit-qubit mutual inductive energy needs to be large and the qubits need to have different single-qubit energy level spacings, i.e. different junction sizes. The latter requirement is consistent with the measurement considerations discussed earlier.

The former requirement represents a tradeoff in the design. If the mutual inductive coupling becomes too strong, the eigenstates of the coupled qubit Hamiltonian are no longer the computational (and measurement states) $|00\rangle$, $|01\rangle$, $|10\rangle$, and $|11\rangle$. Although it is possible to do quantum computation with a system in which the computational states are not the eigenstates, doing so adds much more complexity to the actualization of quantum gate operations. The final requirement on the energy levels is that the energy level differences correspond to readily achievable microwave frequencies. In this case, it makes a difference whether the radiation source is on-chip or off-chip. On-chip radiation sources can more easily be used for frequencies that are several GHz and higher.

Coupled qubits have been designed, simulated, and fabricated at MIT Lincoln Laboratory. In choosing the designs for the coupled qubits, an effort was made to span the available parameter space as much as possible in terms of junction sizes, strength of qubit-qubit coupling, and strength of qubit-SQUID coupling. This approach compensates for manufacturing variability as well as provides a variety in terms of sample characteristics. Measurements on these coupled qubit samples are to begin soon.
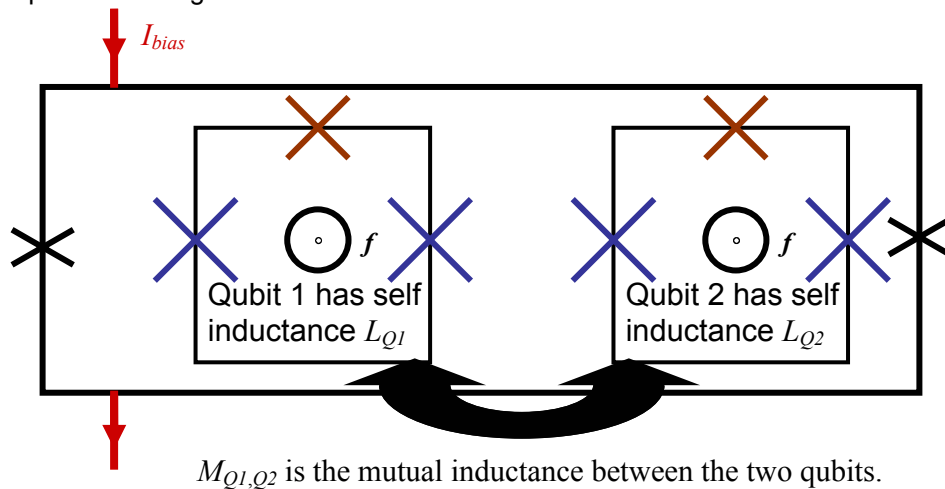

$M_{Q1,Q2}$ is the mutual inductance between the two qubits.
Figure 1: Schematic for coupled PC qubits with a measurement SQUID.

7. Type II Quantum Computing Using Superconducting Qubits

Sponsor

Project Staff
Professor Terry Orlando, David Berns, Professor Karl Berggren, Dr. William Oliver (MIT Lincoln Laboratory), Dr. Jeff Yepez (Air Force Laboratories)

Most algorithms designed for quantum computers will not best their classical counterparts until they are implemented with thousands of qubits. By all measures this technology is far in the future. On the other hand, the factorized quantum lattice-gas algorithm (FQLGA) can be implemented on a type II quantum computer, where its speedups are realizable with qubits numbering only in the teens.

The FQLGA uses a type II architecture, where an array of nodes, each node with only a small number of coherently coupled qubits, is connected classically (incoherently). It is the small number of coupled qubits that will allow this algorithm to be of the first useful quantum algorithms ever implemented.

The algorithm is the quantum mechanical version of the classical lattice-gas algorithm, which can simulate many fluid dynamic equations and conditions with unconditional stability. This algorithm was developed in the 1980's and has been a popular fluid dynamic simulation model ever since. It is a bottom-up model where the microdynamics are governed by only three sets of rules, unrelated to the specific microscopic interactions of the system. The quantum algorithm has all the properties of the classical algorithm but with an exponential speedup in running time.

We have been looking into the feasibility of implementing this algorithm with our superconducting qubits, with long-term plans of constructing a simple type II quantum computer. We currently have a chip scheme to simulate the one dimensional diffusion equation, the simplest fluid dynamics to simulate with this algorithm. The requirements are only two coupled qubits per node, state preparation of each qubit, one two-qubit operation, and subsequent measurement. This can be accomplished with two identical PC qubits inductively coupled, each with microwaves coupled to it (initialization and single qubit rotations during swap operation), and each with a squid around it (measurement). All classical streaming will at first be done off-chip.

8. Scalable Superconducting Architecture for Adiabatic Quantum Computation

Sponsor

Project Staff
William M. Kaminsky, Professor Seth Lloyd, Professor Terry Orlando

Adiabatic quantum computation (AQC) is a recently proposed, general approach to solving computational problems of the complexity class NP via energy minimization [1]. The class NP is of central importance in computational complexity because it includes not only the cryptographic problems like prime factorization thought to be intractable classically yet known to be tractable quantum-mechanically [2], but also virtually every other interesting computational problem that is currently thought to be intractable classically [3]. AQC gets its name from the fact it exploits the ability of coherent quantum systems to follow adiabatically the ground state of a slowly changing Hamiltonian. In so doing, AQC aims to bypass the many separated local minima that occur in difficult minimization problems and confound all known classical algorithms for them. It is still unknown what speedup AQC offers in general over classical algorithms, but most intriguingly, there are indications that typically the speedup is exponential [1, 4–6]. Beyond this obvious theoretical interest, AQC is also of potentially great practical interest because encoding a quantum computation in a single eigenstate, the ground state, offers intrinsic protection against dephasing and dissipation [7, 8].

We have extended the practical interest of AQC by exhibiting a simple, scalable architecture that can handle any class NP problem. Moreover, we have specifically shown how to implement this architecture with present-day superconducting persistent-current (PC) qubits [9–12], which constitute a promising approach to lithographable solid-state qubits. The outline of this architecture was presented in Ref. [13], and full details of its implementation with PC qubits can be obtained in the forthcoming Ref. [14]. The architecture addresses all the major technological obstacles to implementation by being able to tolerate manufacturing imprecision, imperfect measurements, and interqubit couplings that cannot vary during the course of the computation. Moreover, the architecture also highlights two special benefits previously unappreciated about PC qubits and AQC, respectively. First, it shows that it is possible to design inductively coupled flux qubits that can switch from ferromagnetic to antiferromagnetic couplings simply by adjusting the bias fluxes in their loops. Second, it demonstrates that AQC should be able to turn to advantage the classically troublesome fact that frustrated spin systems encoding NP-complete energy minimization problems generically freeze out of equilibrium by turning this endemic fact from something that for all previous algorithms promoted errors into something that prevents them.

The architecture naturally follows from the fact [15] that calculating the ground state of an antiferromagnetically coupled Ising model in a uniform magnetic field is isomorphic to solving the NP-complete graph theory problem Max Independent Set (MIS), which is the problem of finding for a graph $G = (V,E)$ the largest subset S of the vertices V such that no two members of S are joined by an edge from E. Interqubit couplings may be laid on a single plane and kept to a modest number since MIS remains NP-complete even in the ostensibly simple, topologically uniform case of degree-3 planar graphs, *i.e.*, graphs that can be drawn in a plane without any edges crossing and in which every vertex is connected to exactly 3 others [16]. The isomorphism takes a particularly simple form in this case of degree-3 planar graphs: the MISs of a degree-3 planar graph $G = (V,E)$ are the ground states of an Ising model with spins associated with vertices V, equal strength antiferromagnetic couplings associated with edges E, placed in a uniform applied magnetic field along some desired axis. The requirements imposed by technological limitations—nearest neighbor couplings, maximum uniformity, and time independent control—can be readily met via the layout depicted below: a triangular lattice with qubits at its vertices and nearest-neighbor ferro- or antiferromagnetic couplings on its edges. To allow programmability, that is, to embed an arbitrary degree-3 planar graph in this triangular lattice, each coupling is switchable and moreover the magnetic field on each qubit is individually controllable so as to allow one to create "dummy" qubits as desired which possess no single qubit Hamiltonian and act simply to propagate a coupling. (Triangular lattices make it especially easy to embed degree-3 planar graphs, but lattices with a lower node degree, such as square or hexagonal lattices, would also suffice.)
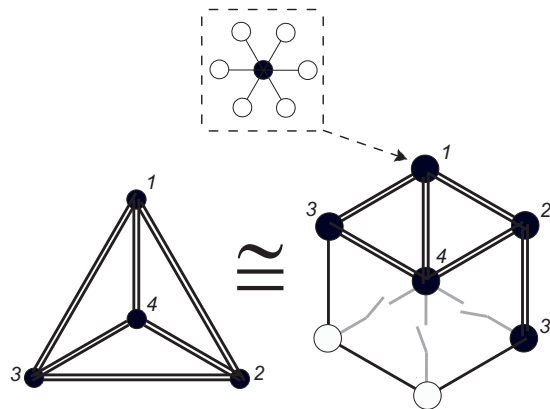

Figure 1: Schematically depicted is the embedding of the simplest degree-3 planar graph (*left*) into the architecture (*right*).

The foundation of the architecture is a triangular lattice with qubits at its vertices (schematically denoted by filled circles if possessing a Zeeman term and thus denoting a graph vertex, open circles if not and thus denoting a dummy vertex that serves only to propagate a coupling) and switchable nearest-neighbor couplings on its edges (schematically denoted by black double lines if antiferromagnetic and switched on, black single lines if ferromagnetic and switched on, and gray broken lines if switched on). This allows an arbitrary degree-3 planar graph to be embedded efficiently within the lattice, as can be seen in how the Qubit #3 of the graph is ferromagnetically coupled via dummies to a partner #3$0$ so that is a nearest neighbor of #2. *Inset*: To compensate for measurement errors, the logical qubits in the architecture (denoted by the larger circles) are actually ferromagnetically coupled clusters of physical qubits (smaller circles). For example, as depicted above, one could ferromagnetically couple 6 dummies to each physical computational qubit and thus essentially compensate for measurement errors by a classical 7-bit repetition code. The ferromagnetic couplings in such redundant clusters need not be switchable.

[1] E. Farhi, J. Goldstone, S. Gutmann, J. Lapan, A. Lundgren, and D. Preda, Science 292, 472 (2001), quant-ph/0104129.
[2] P. W. Shor, in *Proceedings, 35th Annual Symposium on Foundations of Computer Science* (IEEE Press, 1994).
[3] M. G. Garey and D. S. Johnson, *Computers and intractability: a guide to the theory of NP-completeness* (W.H. Freeman and Company, San Francisco, 1979).
[4] A. M. Childs, E. Farhi, J. Goldstone, and S. Gutmann, Quant. Info. Comp. 2, 181 (2002), quant-ph/0012104.
[5] T. Hogg, Phys. Rev. A 67, 022314 (2003), NB: quant-ph/0206059 (v2: Jan 2004) presents simulation data extended to 30 qubits.
[6] E. Farhi, J. Goldstone, and S. Gutmann (2002), quant-ph/0201031.
[7] A. M. Childs, E. Farhi, and J. Preskill, Phys. Rev. A 65, 012322 (2002), quant-ph/0108048.
[8] J. Roland and N. J. Cerf, personal communication (2003).
[9] J. E. Mooij, T. P. Orlando, L. Levitov, L. Tian, C. H. van der Wal, and S. Lloyd, Science 285, 1036 (1999).
[10] T. P. Orlando, J. E. Mooij, L. Tian, C. H. van der Wal, L. S. Levitov, S. Lloyd, and J. J. Mazo, Phys. Rev. B 60, 15398 (1999).
[11] Y. Makhlin, G. Schon, and A. Shnirman, Rev. Mod. Phys. 73, 357 (2001).
[12] G. Burkard, R. H. Koch, and D. P. DiVincenzo, Phys. Rev. B 69, 064503 (2004).
[13] W. M. Kaminsky and S. Lloyd, in *Quantum computing and Quantum Bits in Mesoscopic Systems* (Kluwer Academic, 2003), quant-ph/0211152.
[14] W. M. Kaminsky, S. Lloyd, and T. P. Orlando, forthcoming (2004).
[15] F. Barahona, J. Phys. A 15, 3241 (1982).
[16] M. G. Garey, D. S. Johnson, and L. Stockmeyer, Theo. Comp. Sci. 1, 237 (1976).

9. Probing Decoherence with Electromagnetically Induced Transparency in Superconductive Quantum Circuits

Sponsors

Project Staff
Kota Murali, Dr. Zachary Dutton (NIST), Dr. William Oliver (MIT Lincoln Lab), Donald Crankshaw (University of Rochester), Professor Terry Orlando

Superconductive quantum circuits (SQCs) comprising mesoscopic Josephson junctions can exhibit quantum coherence amongst their macroscopically large degrees of freedom. They exhibit quantized flux and/or charge states depending on their fabrication parameters, and the resultant quantized energy levels are analogous to the quantized internal levels of an atom. Spectroscopy, Rabi oscillation, and Ramsey interferometry experiments have demonstrated that SQCs behave as "artificial atoms" under carefully controlled conditions. The SQC-atom analogy can be extended to another quantum optical effect associated with atoms: electromagnetically induced transparency (EIT). The demonstration of the superconductive analog to EIT (denoted S-EIT) will be in a superconductive circuit exhibiting two meta-stable states (i.e., a qubit) and a third, shorter-lived state (i.e., the readout state). In this setup, S-EIT can be used to experimentally probe the decoherence time of the qubit in a very sensitive manner.

The three-level Λ-system for our S-EIT system (Fig.1a) is a standard energy level structure utilized in atomic EIT. It comprises two meta-stable states $|1\rangle$ and $|2\rangle$, each of which may be coupled to a third excited state $|3\rangle$. In atoms, the meta-stable states are typically hyperfine or Zeeman levels, while state $|3\rangle$ is an excited electronic state that may spontaneously decay (to other unmentioned states) at a relatively fast rate Γ_3. In an atomic EIT scheme, a strong "control" laser couples the $|2\rangle\rightarrow|3\rangle$ transition, and a weak resonant "probe" laser couples the $|1\rangle\rightarrow|3\rangle$ transition.

By itself, the probe laser light is readily absorbed by the atoms and thus the transmittance of the laser light through the atoms is quite low. Similarly, the control laser is also highly absorbed by the atoms. However, when the control and probe laser are applied simultaneously, destructive quantum interference between the atomic states involved in the two driven transitions causes the atom to become "transparent" to both the probe and control laser light. Thus, the light passes through with virtually no absorption. In more recent experiments, ultra-slow light propagation due to EIT-based refractive index modifications in atomic clouds has also been demonstrated.

In our experiments, a persistent-current (PC) qubit will be used as the SQC three-level Λ-system. The PC qubit is a superconductive loop interrupted by two Josephson junctions of equal size and a third junction scaled smaller in area by the factor α, between 0.5 and 1 (Fig. 1b). For flux biases near one-half of a flux quantum, f ~ ½, the potential may be approximated as a double-well, with each well corresponding to a distinct stable classical state of the electric current, i.e., left or right circulation through the loop. In turn, the different current states have net magnetizations in opposite directions, which are measurable with a dc SQUID. As a quantum object, the potential wells exhibit quantized energy levels corresponding to the quantum states of the macroscopic circulating current. These levels may be coupled using microwave radiation, and their quantum coherence has been experimentally demonstrated.

Tuning the flux bias away from f = ½ results in the asymmetric double-well potential illustrated in Fig.1c. The three states in the left well constitute the superconductive analog to the atomic Λ-system. States $|1\rangle$ and $|2\rangle$ are "meta-stable" qubit states, with a tunneling and coherence time much longer than the excited "readout" state $|3\rangle$. State $|3\rangle$ has weakly-coupled intra-well transitions, but has a strong inter-well transition when tuned on-resonance to state $|4\rangle$. Using tight-binding models with experimental PC qubit parameters at a flux bias f=0.5041, we estimate the tunneling times from states $|1\rangle$, $|2\rangle$, and $|3\rangle$ to the right well are $1/\Gamma_1$ ~ 1 ms, $1/\Gamma_2$ ~2 μs, and $1/\Gamma_3$ ~1 ns respectively. Thus, a particle reaching state $|3\rangle$ will tend to tunnel quickly to state $|4\rangle$ causing the circulating current to switch to the other direction, an event that is detected readily with a fast measurement scheme. Alternatively, one may detune states $|3\rangle$ and $|4\rangle$ and then apply a resonant π-pulse to transfer the population from state $|3\rangle$ to $|4\rangle$; since the states are now off-resonance, the relaxation rate back to the left well is reduced and so a slower detection scheme may be used.

In working towards making a practical quantum computer with SQC, the decoherence of the qubit states must be measured, characterized, and minimized. S-EIT is one such sensitive decoherence probe, since even small deviations from perfect destructive interference between the qubit states results in a loss of transparency. Thus, knowing how long the SQC remains transparent (i.e. does not reach state $|3\rangle$) in the S-EIT experiment provides an estimate for the decoherence time.
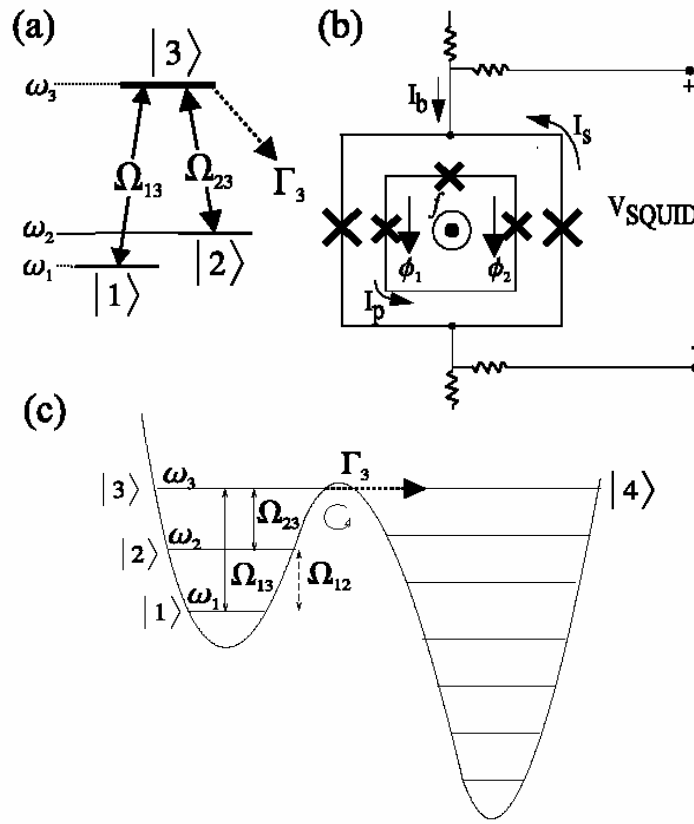
Figure 1: (a) Λ-system generally used for EIT experiments. **(b)** Schematic of DC measurements SQUID and PC Qubit. **(c)** Energy levels in PC Qubit double-well potential.

10. Vortex Ratchets

Personnel
Dr. Kenneth Segall, Dr. Juan Mazo, Professor Terry Orlando

Sponsors
National Science Foundation Grant DMR 9988832, Fulbright/MEC Fellowship

The concept of a *ratchet* and the *ratchet effect* has received attention in recent years in a wide variety of fields. Simply put a ratchet is formed by a particle in a potential which is asymmetric, i.e. it lacks reflection symmetry. An example is the potential shown in Fig.1, where the force to move a particle trapped in the potential is larger in the left (minus) direction and smaller in the right (plus) direction.   The ratchet effect is when net transport of the particle occurs in the absence of any gradients. The transport is driven by fluctuations. This can happen when the system is driven out of equilibrium, such as by an unbiased AC force or non-gaussian noise. Ratchets are of fundamental importance in biological fields, for study of dissipation and stochastic resonance, in mesoscopic systems, and in our case in superconducting Josephson systems. The key questions are to study how the ratchet potential affects the transport of the particle.

In our group we study the ratchet effect in circular arrays of superconducting Josephson Junctions. In such arrays magnetic vortices or kinks can be trapped inside and feel a force when the array is driven by an external current. The potential that the vortex feels is given by a combination of the junction sizes and the cell areas; by varying these in an asymmetric fashion we can construct a ratchet potential for a vortex. The picture in Fig. 1 is of one of our fabricated circular arrays; the potential shown in Fig. 1 is the numerically calculated potential for a kink inside the array. We have verified the ratchet nature of the potential with DC transport measurements, published in early 2000.

This work is now moving in the quantum direction: smaller junction arrays where quantum effects are important. A quantum ratchet will display new behavior as the temperature is lowered, as both the ratchet potential and quantum tunneling can contribute to the kink transport. We have designed and fabricated such arrays and are presently testing them. The experiments we do in these newer devices is to measure the switching current, which is the current that is required to cause the vortex to depin and the system to switch to a running mode or finite voltage state. In the mechanical analog it represents the critical force to move the particle, and in a ratchet potential it is different in one direction than the other. For a classical ratchet, the direction with the lower critical force will always have the larger depinning rate. However, in a quantum ratchet the direction with the lower transition rate will depend on the temperature. A crossover in the preferred direction, the direction with the larger depinning rate, is the signature of possible quantum behavior. In Fig. 2 we show the switching current as a function of temperature for the two directions. A crossover is clearly seen. We are in the process of doing further experiments and calculations to verify that we have truly made a quantum ratchet.
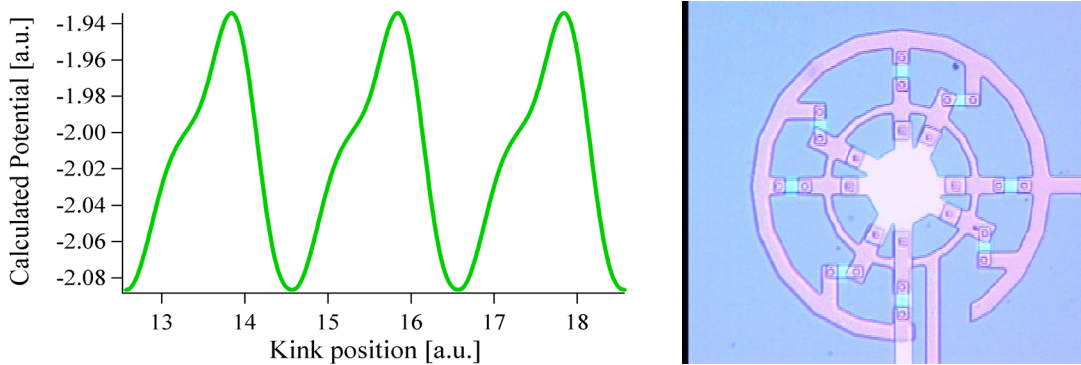

Figure 1: A ratchet potential and its realization in a Josephson array. The array has alternating junction sizes and plaquete areas to form the asymmetric potential for a vortex trapped inside the ring. The outer ring applies the current such that the vortex transport can be measured. The potential is numerically calculated for the array parameters.
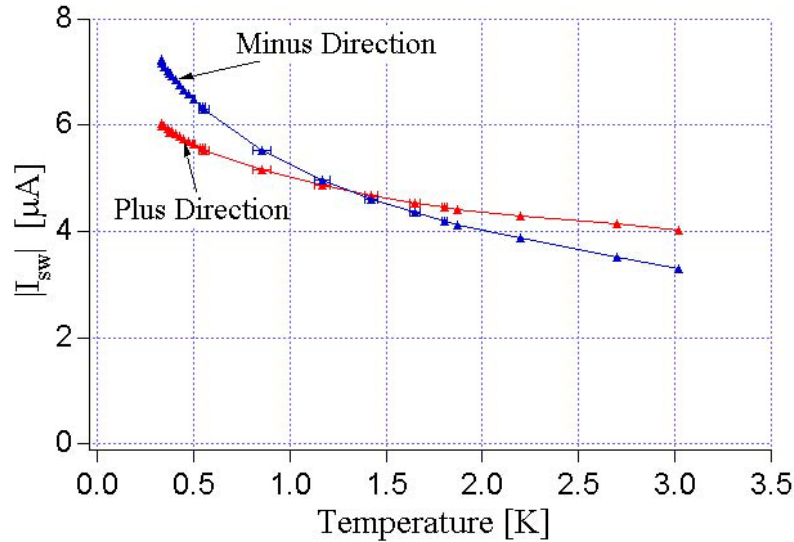
Figure 2: Switching current for the plus and minus direction of a circular, 1-D Josephson array fabricated in the quantum regime. The switching current is a measure of the depinning rate in each direction. The crossover indicates that the preferred direction changes as a function of temperature. This is a possible signature of quantum effects.

Journal Articles, Published

D.S. Crankshaw, Dr. K. Segall, D. Nakada, T.P. Orlando, L.S. Levitov, S. Lloyd, S.O. Valenzuela, N. Markovic, M. Tinkham, K.K. Berggren, "DC Spectroscopy of Macroscopic Quantum Levels in a Superconducting Qubit Structure with a Time-Ordered Meter," *Phys. Rev. B* (2004), forthcoming.

Yang Yu, D. Nakada, Janice Lee, B. Singh, D. Crankshaw, T. P. Orlando, William Oliver, Karl K. Berggren, "Energy Relaxation Time between Macroscopic Quantum Levels in a Superconducting Persistent Current Qubit," *Phys. Rev. Lett.* 92 (11): 117904-1-4 (2004).

Daniel Nakada, Karl K. Berggren, Earl Macedo, Vladimir Liberman, Terry P. Orlando, "Improved Critical-Current-Density Uniformity by Using Anodization," *IEEE Transaction of Applied Superconductivity* 13 (2): 111-114 (2003).

D. Nakada, K.K. Berggren, E. Macedo, V. Liberman, T.P. Orlando, "Improved Critical-Current-Density Uniformity by Using Anodization," *IEEE Transaction of Applied Superconductivity* 13(2): 111-4 (2003).

D.S. Crankshaw, *Measurement and On-chip Control of a Niobium Persistent Current Qubit*, PhD thesis, MIT, 2003.

D.S. Crankshaw, J.L. Habif, X.X. Zhou, T.P. Orlando, M.J. Feldman, M.F. Bocko, "An RSFQ Variable Duty Cycle Oscillator for Driving a Superconductive Qubit, " *IEEE Transaction of Applied Superconductivity* 13(2): 966-969 (2003).

J.J. Mazo, T.P. Orlando, "Discrete Breathers in Josephson Arrays," *Choas* 13: 733-743 (2003).

K. Segall, D.S. Crankshaw, D. Nakada, T.P. Orlando, L.S. Levitov, S. Lloyd, M. Tinkham, N. Markovic, S. Valenzuela, and K.K. Berggren, "Impact of Time-Ordered Measurements of the Two States in a Niobium Superconducting Qubit Structure," *Phys. Rev. B Rapid Communications* 67: 220506-1-4   (2003).

K. Segall, D.S. Crankshaw, D. Nakada, B. Singh, J. Lee, T.P. Orlando, K.K. Berggren, N. Markovic, S.O. Valenzuela, and M. Tinkham, "Experimental Characterization of the Two Current States in a Nb Persistent-Current Qubit," *IEEE Transaction of Applied Superconductivity* 13(2): 1009-12 (2003).

K. Segal, D. Crankshaw, D. Nakada, T.P. Orlando, L.S. Levitov, S. Lloyd, N. Markovic, S.O. Valenzuela, M. Tinkham, K.K. Berggren, "Impact of Time-Ordered Measurements of the Two Sates in a Niobium Superconducting Qubit Structure," *Phys. Rev. B* 67: 220506 (2003).

K. V. R. M. Murali, D. S. Crankshaw, T. P. Orlando, Z. Dutton, W. D. Oliver, "Probing Decoherence with Electromagnetically Induced Transparency in Superconductive Quantum Circuits," *Phys. Rev. Lett.* (2003).

Lin Tian, Seth Lloyd, and T. P. Orlando, "Projective Measurement Scheme for Solid-State Qubits," *Physical Review B* 67: 220505-1-4 (2003).

William M. Kaminsky and Seth Lloyd, "Scalable Architecture for Adiabatic Quantum Computing of NP-hard problems, in Quantum computing and Quantum Bits in Mesoscopic Systems," *Kluwer Academic* (2003).

Yang Yu and Siyuan Han, "Resonant escape over an oscillating barrier in under-damped Josephson tunnel junctions," *Phys. Rev. Lett.* 91: 127003 (2003).

F. Falo , P.J. Martinez, J.J. Mazo, T.P. Orlando, K. Segall, E. Trias, "Fluxon Ratchet Potentials in Superconducting Circuits," *Applied Physics A-Materials Science & Processing* 75: 263-269 (2002).

L. Tian, S. Lloyd and T.P. Orlando, "Decoherence and Relaxation of Superconducting Persistent-Current Qubit During Measurement, " *Phys. Rev. B* 65: 144516-1-7 (2002).

T.P. Orlando, Lin Tian, D.S. Crankshaw, S. Lloyd, C.H. van der Wal, J.E. Mooij, F. Wilhelm, "Engineering the Quantum Measurement Process for the Persistent Current Qubit," *Physica C* 368: 294-299 (2002).

T.P. Orlando, S. Lloyd, L.S. Levitov, K.K. Berggren, M.J. Feldman, M.F. Bocko, J.E. Mooij, C.J.P. Harmans, C.H. van der Wal, "Flux-Based Superconducting Qubits for Quantum Computation," *Physica C-Superconductivity and Its Applications* 372: 194-200 (2002).